The Plant Cell, Vol. 19: 226–236, January 2007, www.plantcell.org

The Kinesin ATK5 Functions in Early Spindle Assembly in *Arabidopsis* [W]

J. Christian Ambrose and Richard Cyr[1]

Department of Biology, Huck Institutes of the Life Sciences, Integrative Biosciences Graduate Degree Program, Plant Physiology Program, Pennsylvania State University, University Park, Pennsylvania 16802

During cell division, the mitotic spindle partitions chromosomes into daughter nuclei. In higher plants, the molecular mechanisms governing spindle assembly and function remain largely unexplored. Here, live cell imaging of mitosis in *Arabidopsis thaliana* plants lacking a kinesin-14 (ATK5) reveals defects during early spindle formation. Beginning during prophase and lasting until late prometaphase, spindles of *atk5-1* plants become abnormally elongated, are frequently bent, and have splayed poles by prometaphase. The period of spindle elongation during prophase and prometaphase is prolonged in *atk5-1* cells. Time-lapse imaging of yellow fluorescent protein:ATK5 reveals colocalization with perinuclear microtubules before nuclear envelope breakdown, after which it congresses inward from the poles to the midzone, where it becomes progressively enriched at regions of overlap between antiparallel microtubules. In vitro microtubule motility assays demonstrate that in the presence of ATK5, two microtubules encountering one another at an angle can interact and coalign, forming a linear bundle. These data indicate that ATK5 participates in the search and capture of antiparallel interpolar microtubules, where it aids in generating force to coalign microtubules, thereby affecting spindle length, width, and integrity.

INTRODUCTION

Cell division is a fundamental process governing the central elements of plant growth and development. A key event in cell division is the formation of the mitotic spindle apparatus, an array of microtubules (MTs) and MT-associated proteins responsible for the segregation of chromosomes into daughter nuclei. In addition to the intrinsic dynamic properties of MTs, several families of kinesin motor proteins are essential players governing spindle assembly and function. Kinesins undergo ATP-dependent conformational changes in the conserved motor domain that drive translocation along MTs, whereas the variable tail domain interacts with cellular cargos to facilitate their transport to appropriate subcellular destinations. In animals and fungi, eight of the 14 families of kinesins have been implicated in various aspects of mitosis and/or meiosis (Goshima and Vale, 2003; Zhu et al., 2005); however, comparatively little is known in plants. The lack of discrete MT organizing centers (Murata et al., 2005) and dynein motor proteins in higher plants (Arabidopsis Genome Initiative, 2000) suggests that kinesins likely make a large contribution to spindle organization. Accordingly, *Arabidopsis thaliana* contains 61 predicted kinesins, one-third of which belong to the kinesin-14 family. This study focuses on the kinesin-14 family, which comprises the sole group of minus end–directed kinesins (McDonald et al., 1990; Walker et al., 1990; Dagenbach and Endow, 2004).

Kinesin-14 family members contain a C-terminal motor domain that confers nonprocessive motility to the MT minus end, and several members have an additional MT binding site located in the N-terminal tail (Narasimhulu and Reddy, 1998; Karabay and Walker, 1999). The presence of distinct motor and tail MT binding sites confers the ability to cross-link and slide MTs relative to one another (Surrey et al., 2001), making kinesin-14 family members adaptive for mediating MT–MT interactions in the spindle. Kinesin-14 family members function in two ways in the spindle: (1) cross-linking of parallel MTs in each half-spindle, where they focus minus ends into poles (Matthies et al., 1996; Walczak et al., 1998; Chen et al., 2002; Goshima and Vale, 2003); and (2) cross-linking of antiparallel MTs near the spindle midzone and sliding them together, thereby generating inward forces between spindle halves to counterbalance the outward forces produced by kinesin-5 motors (O'Connell et al., 1993; Mountain et al., 1999; Sharp et al., 1999). In plants, evidence has been presented for pole-focusing forces (Smirnova et al., 1998; Chen et al., 2002); however, no direct functional evidence has yet been reported for the generation of inward forces.

We previously showed that the kinesin-14 family member ATK5 is a plus end tracking protein that localizes to mitotic spindles with enrichment in the midzone, where it generates forces resulting in lateral compaction of the spindle during metaphase and anaphase (Ambrose et al., 2005). Here, live cell imaging reveals that plants lacking ATK5 exhibit additional defects in early spindle assembly consistent with losses of pole focusing and inward forces. Spindles of *atk5-1* null mutant plants are bent and abnormally elongated with splayed poles during prometaphase, and the duration of prophase/prometaphase is prolonged. Imaging of yellow fluorescent protein (YFP):ATK5

[1] To whom correspondence should be addressed. E-mail rjc8@psu.edu; fax 814-865-9131.

The author responsible for distribution of materials integral to the findings presented in this article in accordance with the policy described in the Instructions for Authors (www.plantcell.org) is: Richard Cyr (rjc8@psu.edu).

[W] Online version contains Web-only data.

www.plantcell.org/cgi/doi/10.1105/tpc.106.047613

during the prophase-to-prometaphase transition reveals its localization and enrichment in regions of overlap between interpolar MTs. In vitro motility assays demonstrate the ability of ATK5 to coalign MTs into linear bundles, providing a mechanism for ATK5-dependent spindle compaction and straightening. We hypothesize that ATK5 mediates lateral interactions between spindle MTs, where it uses minus end motility to generate inward forces and coalign MTs into linear bundles. These lateral interactions in turn foster spindle compaction and increase the structural integrity of the spindle at the poles and the midzone.

RESULTS

Live Imaging of *atk5-1* Null Spindles Reveals Defects in Spindle Formation

Previous studies using tubulin immunofluorescence on *atk5-1* cells revealed laterally broadened mitotic spindles during metaphase and anaphase (Ambrose et al., 2005). The midzone accumulation of YFP:ATK5 was in accordance with broadening at the spindle midzone, although it was unclear how the spindle poles also became splayed. To understand how ATK5 contributes to spindle pole integrity, we stably transformed wild-type and *atk5-1* plants with a chimeric gene construct harboring a fusion between green fluorescent protein (GFP) and *Arabidopsis* β-Tubulin6 (TUB6) and used plants with detectable levels of fluorescence in dividing cells of the root tip for high-spatiotemporal-resolution imaging of spindle formation and function. All transgenic plants exhibited normal morphologies and growth parameters, and the structure and function of MT arrays were not noticeably affected over a range of transgene expression levels.

Figure 1 shows the progression through mitosis in a representative cell from wild-type root tips (see Supplemental Movie 1 online), which supports documented observations. During late G2/early prophase in typical wild-type cells, a broad preprophase band (PPB) of MTs forms beneath the cortex encircling the nucleus and progressively narrows as the cell approaches the onset of mitosis (Wick and Duniec, 1983; Vos et al., 2004). Concurrent with PPB narrowing, MTs appear in the vicinity of the nuclear envelope and subsequently become distributed into two poles on opposite sides of the nucleus to form the prophase spindle, the axis of which is perpendicular to the plane of the PPB (Baskin and Cande, 1990; Mineyuki et al., 1991; Nogami et al., 1996). MTs emanating from these poles are oriented tangentially to the nuclear surface and extend along the surface of the nucleus to the equatorial region, where they overlap with MTs from the opposite pole, or they extend laterally and interact with the PPB (Mineyuki et al., 1991; Nogami et al., 1996). Soon after pole formation, the prophase spindle begins elongating in a

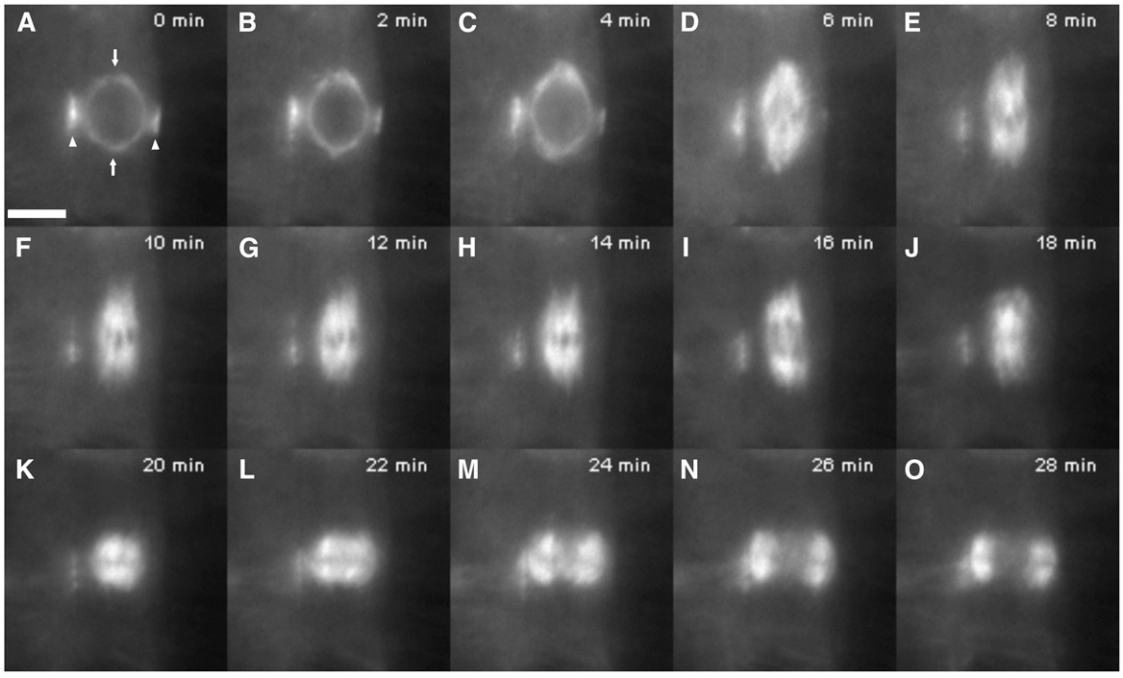

Figure 1. Mitosis in a Wild-Type *Arabidopsis* Plant Expressing GFP:TUB6.

Images are taken from a time-lapse series (see Supplemental Movie 1 online).
(A) Prophase spindle with narrow PPB. Arrowheads indicate PPB, and arrows indicate incipient spindle poles. Bar = 5 μm.
(B) and **(C)** Prophase spindle elongation **(B)** and NEB **(C)**.
(D) and **(E)** Prometaphase.
(F) to **(H)** Metaphase.
(I) Anaphase.
(J) to **(O)** Telophase/cytokinesis, showing the phragmoplast expanding centrifugally.

direction parallel to its long axis (Figures 1B to 1E). This elongation continues through nuclear envelope breakdown (NEB), with the spindle achieving maximum length during prometaphase, after which MTs congress inward to form the metaphase spindle (Figures 1F to 1H). After anaphase (Figure 1I) is completed, MTs congress back to the equatorial region to give rise to the phragmoplast (Figures 1J to 1O), which deposits cell plate material as it expands outward.

Figure 2 shows the progression through mitosis in a representative cell from *atk5-1* root tips (see Supplemental Movie 2 online). Beginning during prophase spindle elongation and lasting until the end of prometaphase, spindles of *atk5-1* cells become abnormally elongated with splayed spindle poles and often display a bent morphology (Figures 2A to 2I). Throughout prophase spindle elongation, the mean pole-to-pole spindle length is significantly greater in *atk5-1* spindles compared with the corresponding stage in wild-type spindles (Figures 2A to 2F). This difference becomes more pronounced as cells progress into prometaphase (Figures 2F to 2I); however, by metaphase, mutant spindles have shortened to lengths similar to wild-type spindles (Figures 2J to 2M).

Mean *atk5-1* spindle length during late prophase (just before NEB) is 9.8 $\pm$ 0.3 μm ($n = 32$) versus 8.4 $\pm$ 0.3 μm in wild-type cells ($n = 31$; $P = 4.0 \times 10^{-9}$ by Student's *t* test). During prometaphase (i.e., after NEB but before the establishment of a clear metaphase plate), mean spindle length increases to 11.0 $\pm$ 0.1 μm ($n = 37$) in *atk5-1* cells versus 9.3 $\pm$ 0.3 μm in wild-type cells ($n = 32$; $P = 1.5 \times 10^{-11}$ by Student's *t* test). During metaphase and anaphase, *atk5-1* spindle lengths are not significantly different from those of the wild type.

In agreement with our previous results using tubulin immunofluorescence, metaphase and anaphase spindles in *atk5-1* plants

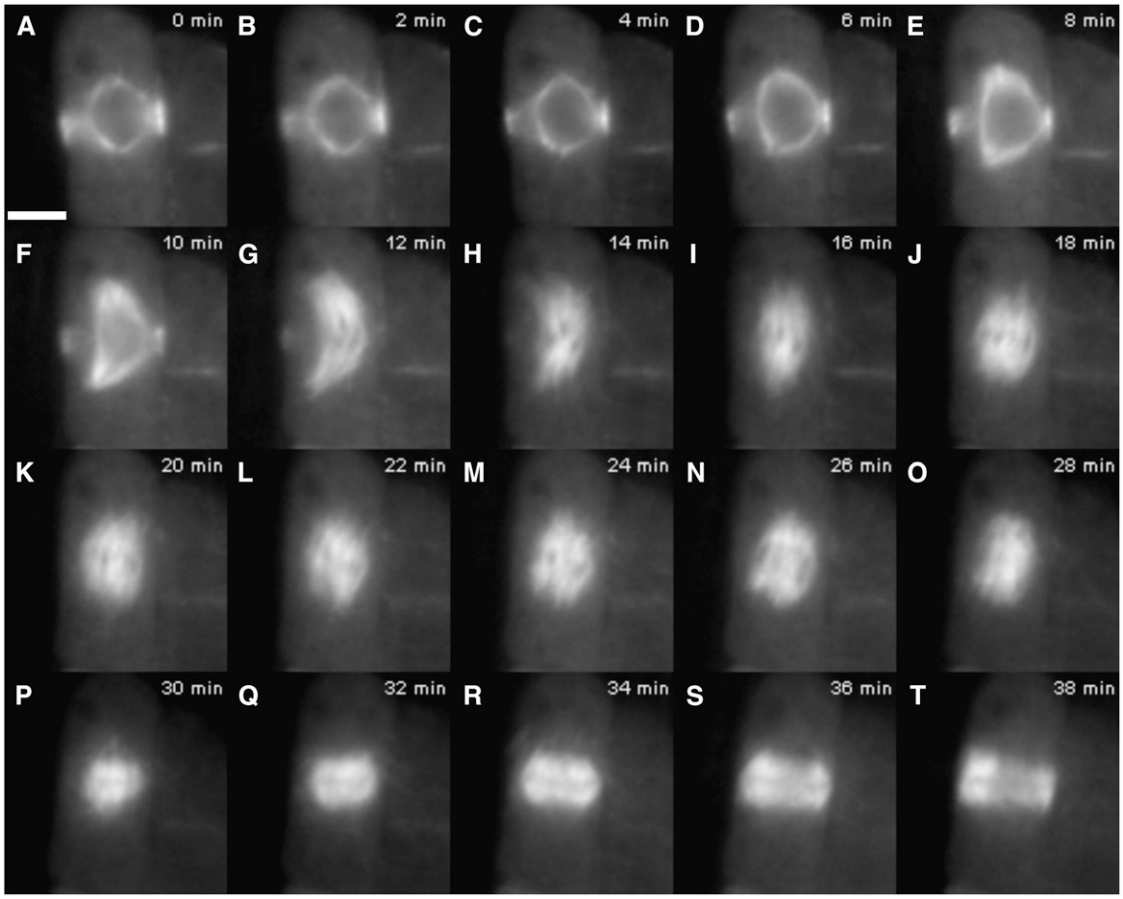

Figure 2. Aberrant Mitosis in an *atk5-1* Plant Expressing GFP:TUB6.

Images are taken from a time-lapse series (see Supplemental Movie 2 online).
(A) Prophase spindle with PPB. Bar = 5 μm.
(B) to **(E)** Prophase spindle elongation and NEB.
(F) to **(I)** Prometaphase.
(J) to **(M)** Metaphase.
(N) Anaphase.
(O) to **(T)** Telophase/cytokinesis.

are significantly wider at the midzone and poles (Figures 2M to 2O). Here, we observed that this broadening manifested first as a splaying of the poles during prometaphase, then later at the midzone during metaphase. At prometaphase, *atk5-1* spindle poles are broader than those of the wild type, whereas the width measured at the spindle midzone is not significantly different at this stage. The mean spindle width, measured at the poles, was found to be 2.8 ± 0.1 μm ($n = 37$) for *atk5-1* and 2.0 ± 0.2 μm for the wild type ($n = 32$; $P = 2.1 \times 10^{-6}$ by Student's *t* test), whereas the mean midzone width was 4.5 ± 0.1 μm for *atk5-1* and 4.6 ± 0.1 μm for the wild type.

During prometaphase and metaphase, spindles of *atk5-1* also exhibit less structural integrity than those of the wild type. Wild-type spindles maintain an ordered appearance, with little noticeable movement of the well-aligned kinetochore fibers, whereas *atk5-1* spindles appear much more disorganized, with individual kinetochore fibers displaying a greater degree of autonomy and movement during metaphase (Figures 2G to 2M; see Supplemental Movies 1 and 2 online). This is most evident at the broadened poles of *atk5-1* spindles, which appear highly disorganized and unstable. Overall, *atk5-1* spindles appear deficient in lateral interactions between neighboring kinetochore bundles, resulting in broader and less compact spindle structure compared with wild-type spindles.

atk5-1 Mutant Spindles Exhibit an Increased Duration of Prophase/Prometaphase Spindle Elongation

In addition to elongated prophase/prometaphase spindles, the duration of this stage is significantly extended in *atk5-1* (Table 1). Measuring the time from the start of prophase spindle elongation until the maximum length is reached during prometaphase, spindles from *atk5-1* cells elongate for an average of 9.9 ± 2.9 min versus 5.8 ± 1.9 min in wild-type cells. A slight increase in the duration between prometaphase and anaphase is also observed (Table 1). As shown in Figure 3, the rate of spindle elongation appeared normal in *atk5-1* cells (0.7 ± 0.2 μm/min), suggesting that this increased duration of prophase/prometaphase is not attributable to slowed separation of poles but instead is the result of an extended period of elongation. To test whether this increased duration was caused by a premature initiation or delayed termination of spindle elongation, the PPB was used as a marker for mitotic status, because its width decreases in a timely and predictable manner as the spindle develops (Mineyuki et al., 1991; Vos et al., 2004). To determine whether prophase spindle elongation began earlier in *atk5-1* cells, PPB widths were measured at the start of prophase spindle elongation. PPB widths are significantly greater at this stage in *atk5-1* compared with the wild type (2.3 ± 0.3 μm for *atk5-1* [$n = 42$] and 1.9 ± 0.4 μm for the wild type [$n = 45$]; $P = 0.0002$ by Student's *t* test), suggesting that elongation starts early in *atk5-1* cells. Additionally, maximum prometaphase spindle lengths were seen to coincide with PPB disappearance in both *atk5-1* and the wild type, further indicating that spindle elongation ended at the normal time and did not extend further. Lastly, in *atk5-1* cells, spindle elongation was seen to begin coincident with the establishment of prophase spindle bipolarity, whereas an accumulation of MTs at the poles was evident before spindle elongation in wild-type cells. Anaphase duration and spindle elongation rates are unaffected in *atk5-1* spindles.

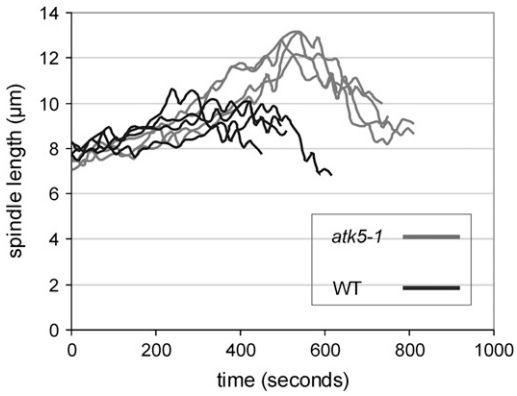

Figure 3. Spindles of *atk5-1* Plants Exhibit an Increased Duration of Prophase/Prometaphase Spindle Elongation.

Spindle lengths from four cells of the wild type (black lines) and *atk5-1* (gray lines) were measured every 15 s during prophase/prometaphase spindle elongation. The peak of each line represents maximum prometaphase spindle length, after which MTs congress inward to the equator to form the metaphase spindle.

Table 1. Kinetics of Mitotic Spindle Development

Genotype	Prophase/Prometaphase Spindle Elongation Time (min)	Prometaphase-to-Anaphase Time (min)	Cells (*n*)
Wild type	5.8 ± 1.9	8.6 ± 1.4	24
atk5-1	9.9 ± 2.9	7.7 ± 1.9	21
	$P = 5.7\ e^{-7}$	$P = 0.027$	

Times are means ± SD. Prophase/prometaphase spindle elongation is defined as the point from the first noticeable elongation of the prophase spindle until the maximum length is reached at prometaphase. Prometaphase to anaphase is defined as the time from maximum prometaphase length until the first noticeable anaphase spindle elongation. P values were determined with Student's *t* test.

ATK5 Is Enriched at Overlapping Regions of Early Interpolar MTs

Because live imaging of mitosis in *atk5-1* cells revealed defects in prophase/prometaphase spindle formation, we sought to explore the dynamic changes of ATK5 localization in dividing cells specifically at this stage to better understand the site(s) of ATK5 force generation. Therefore, we used *Arabidopsis* plants stably expressing a YFP:ATK5 fusion protein. Previous work showed that this fusion protein tracks MT plus ends during interphase, exhibits minus end motility in vitro, and localizes to mitotic spindle midzones in tobacco (*Nicotiana tabacum*) BY-2 cells (Ambrose et al., 2005). All lines analyzed expressed low levels of transgene (as indicated by weak fluorescence signal and low signal:noise ratio) and did not affect the morphology or behavior of MT arrays (see Supplemental Table 1 online). The YFP:ATK5

chimeric protein can function in vivo, as homozygous *atk5-1* plants expressing YFP:ATK5 show a significant decrease in spindle lengths compared with untransformed mutant plants (4.4 μm compared with 5.2 μm in mutants; $P = 0.000001$ by Student's *t* test). Figure 4 shows frames from a time series depicting the localization of YFP:ATK5 in a mitotic cell from a wild-type *Arabidopsis* root tip. During prophase, YFP:ATK5 localizes to MTs of the PPB and prophase spindle (Figures 4A to 4D). As the prophase spindle elongates and progresses to prometaphase, YFP:ATK5 localizes to MTs of the fusiform spindle and becomes progressively enriched on MT bundles overlapping the spindle midzone while simultaneously becoming depleted at the poles (Figures 4E to 4I). By metaphase, the spindle poles have broadened and YFP:ATK5 is concentrated predominantly in the spindle midzone (Figures 4J to 4L). This steady shift in YFP:ATK5 accumulation from poles to the midzone during spindle formation provides an explanation of the gradual broadening of poles seen in *Arabidopsis* spindles as they approach metaphase. These data show localization of ATK5 to early prometaphase spindle midzones, presumably before a substantial number of kinetochore fibers have formed, suggesting that ATK5 force generation during prometaphase occurs at regions of overlap between antiparallel interpolar MTs.

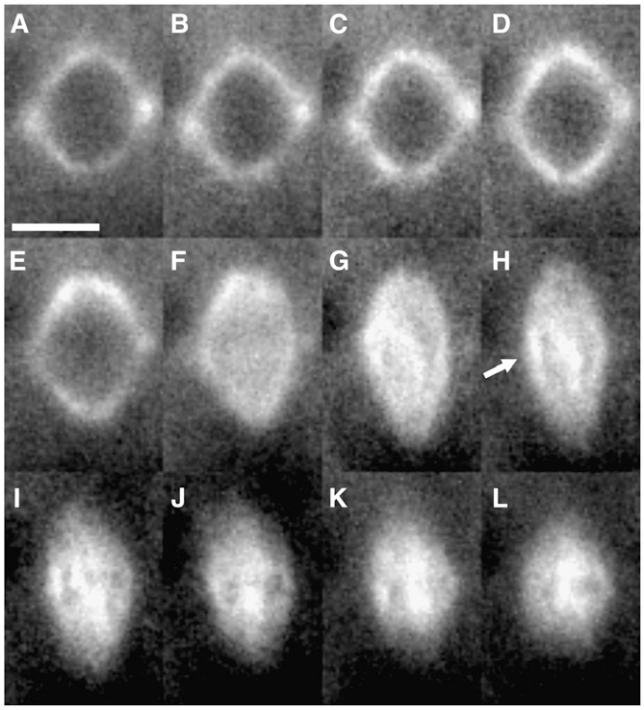

Figure 4. Time Series of YFP:ATK5 Localization during Mitotic Spindle Formation in an *Arabidopsis* Root Tip Cell.

(A) and **(B)** Prophase spindle. YFP:ATK5 localizes to MTs of the prophase spindle and PPB. Bar = 5 μm.
(C) to **(E)** Prophase spindle elongation.
(F) NEB.
(G) to **(I)** Prometaphase.
(J) to **(L)** Metaphase.
After NEB **(F)**, YFP:ATK5 becomes enriched on interpolar MT bundles traversing the midzone (arrow in **[H]**). Intervals between frames are 1 min.

To test the hypothesis that YFP:ATK5 localizes to interpolar MTs during the prophase/prometaphase transition, we analyzed YFP:ATK5 dynamics in a tobacco BY-2 cell line harboring an MBD:Ds Red fusion protein, which is used to visualize MTs (Dixit and Cyr, 2004). BY-2 cells were chosen because of their large spindles and substantial midzones, making them well suited for studies requiring high spatiotemporal resolution. Before NEB, a fusiform prophase spindle encapsulates the nucleus and contains numerous MT connections to the narrow PPB. Distinct from the situation observed in *Arabidopsis* cells, spindles of BY-2 cells do not undergo significant prophase/prometaphase spindle elongation. Instead, at NEB/prometaphase, the MTs congress inward from the poles to the midzone, where they are organized into a barrel-shaped metaphase spindle. Figure 5 shows frames from a time-lapse series of a BY-2 cell expressing YFP:ATK5 and MBD:Ds Red during the transition from prophase to prometaphase (see Supplemental Movie 3 online). Fluorescence intensity profiles to the right of each time point were derived from a line drawn along the pole-to-pole axis of each merged image. Dual imaging reveals that YFP:ATK5 initially colocalizes with all spindle MTs during prophase (Figure 5, 0 min). As the nuclear envelope breaks down and MTs congress to the equator (Figure 5, 2.5 min), YFP:ATK5 appears on thick MT bundles that span the midzone, where it subsequently becomes progressively enriched relative to MTs throughout the sequence (Figure 5, 5 to 7.5 min). Coincident with this midzone accumulation of fluorescence, a proportionate depletion of fluorescence occurs at the poles while the MT signal remains predominantly polar.

The midzone-spanning MT bundles appear stable, as judged by the ability to observe individual bundles for several successive frames (see Supplemental Movie 3 online), often exhibiting pronounced lateral movement within the spindle. These bundles are most likely interpolar MT bundles, because they cross the midzone as a continuous entity rather than becoming interrupted by a kinetochore and because they do not exhibit the characteristic fir tree morphology of plant kinetochore bundles (Bajer and Molè-Bajer, 1986; Palevitz, 1988). With respect to the pattern of accumulation of YFP:ATK5 in the midzone, examination of Supplemental Movie 3 online gives the impression that YFP:ATK5 fluorescence moves on MT bundles from its initial location at the poles to the midzone during prometaphase (although the high density of MTs in this cell made this difficult to document in a static figure). Figure 6 shows a more favorable cell illustrating this inward movement. The more sparsely populated midzone during early prometaphase in this cell exposed the movement of individual MT bundles more readily.

Figure 6A shows frames from a time-lapse series (15-s intervals between frames) of the transition from prophase to prometaphase in a BY-2 cell expressing YFP:ATK5 and MBD:Ds Red (see Supplemental Movie 4 online). Again, YFP:ATK5 initially colocalized with all spindle MTs during prophase (Figure 6A, first frame) and became progressively enriched in the midzone, relative to MTs throughout early prometaphase. Significantly, we noticed that when two bundles from opposite poles encountered each other and coaligned, YFP:ATK5 became enriched at the regions of overlap (asterisks in Figure 6A). In this sequence, two of these

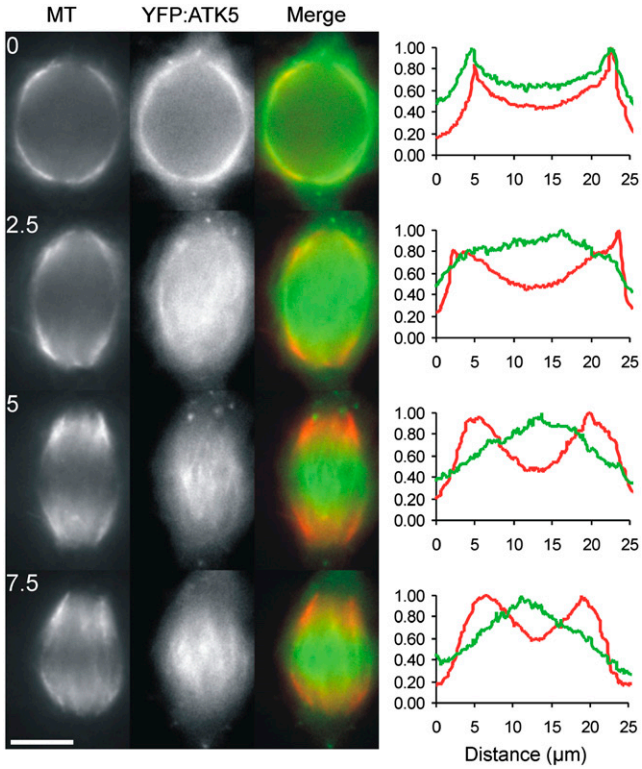

Figure 5. Localization of YFP:ATK5 (Green) during the Transition from Prophase to Early Prometaphase in a Tobacco BY-2 Cell Expressing MBD:Ds Red (Red) as a MT Reporter.

Images are taken from a time-lapse series at 2.5-min intervals (see Supplemental Movie 3 online). Fluorescence intensity profiles for each time point correspond to absolute pixel values for each fluorophore on a line drawn along the long axis of the spindle (MTs = red, YFP:ATK5 = green). At 0 min, YFP:ATK5 colocalizes evenly with MTs of the prophase spindle, which surrounds the nucleus. After NEB, YFP:ATK5 becomes progressively enriched on interpolar MT bundles spanning the midzone while becoming proportionately depleted from the poles relative to MT fluorescence (2.5 to 7.5 min). Bar = 10 μm.

capture events occur: the first, at 75 s, establishes an interpolar MT bundle; the second, at 175 s, reveals the capture and subsequent incorporation of another MT into this same bundle. A kymograph of this time-lapse series taken along the long axis of the spindle (indicated by a dotted line in the first frame) clearly illustrates the relationship between MTs and YFP:ATK5 fluorescence from prophase to prometaphase (Figure 6B). Notably, the YFP:ATK5 signal moves from pole to midzone during early prometaphase. These data suggest that ATK5 moves from the poles to the midzone on early nonkinetochore MTs and becomes enriched at regions of overlap between antiparallel-oriented MTs as interpolar MT connections are established.

ATK5 Rectifies Discordant MT Orientation in Vitro

The observation that ATK5 localized to regions of overlap between antiparallel interpolar MT bundles in the midzone led us to hypothesize that ATK5 mediates lateral MT–MT interactions. To test this hypothesis, ATK5 was expressed as a glutathione *S*-transferase (GST) fusion protein in bacteria as described (Ambrose et al., 2005), and GST:ATK5-containing cleared bacterial lysates were used for in vitro studies. Consistent with observations of several other kinesin-14 family members, significant bundling of rhodamine-labeled MTs was seen to occur in the presence of GST:ATK5 and ATP (see Supplemental Figure 1 online). This bundling was not observed with supernatants expressing GST alone (see Supplemental Figure 1 online).

To observe the formation of these bundles, a modified MT gliding assay was used in which MTs were mixed with GST:ATK5 to allow association with MTs in solution before observation on glass slides. When the solution of GST:ATK5 and MTs was injected into flow cells, gliding of single MTs as well as linear MT bundles along the GST:ATK5-coated surface was observed. Over time, the proportion of MTs residing within bundles increased, as did bundle size. The formation of linear bundles is shown in Figure 7, wherein single MTs interact and subsequently coalign. Figure 7A shows two MTs in antiparallel orientation (inferred from the direction of MT gliding), whereas Figure 7B shows two parallel MTs. In both cases, MTs glided along the ATK5-coated cover slip, and upon encounter, interacted to form a linear bundle. Notably, even when MTs approached one another along different angles of trajectory, upon encounter, subsequent motility became oriented to a common vector, resulting in linear coalignment. The net result is a loss of angle between two MTs as they are aligned along a common axis.

DISCUSSION

ATK5 Functions during Mitosis

Higher plants contain a large number of kinesins, compared with other taxonomic groups, and a large proportion of these belong to the kinesin-14 family (Richardson et al., 2006). One idea that may explain this abundance is the great diversity of cell cycle–dependent MT configurations found in plants and the absence of discrete MT organizing centers, which may necessitate a greater role for motor protein–based MT organization. In a previous study, we showed that ATK5 localizes to spindle midzones during metaphase and anaphase, where it generates lateral compaction of spindle MTs (Ambrose et al., 2005). It was hypothesized that ATK5 functions by linking MTs with different angles and coaligning them into a linear bundle, the overall effect being narrowing of the spindle. In this study, we confirm the ability of ATK5 to coalign gliding MTs into linear bundles in vitro and provide further evidence in support of this notion in vivo. Specifically, the presence of bent prophase/prometaphase spindles in *atk5-1* plants and the enrichment of YFP:ATK5 on regions of overlap between antiparallel MTs suggest a mechanistic model wherein ATK5 mediates lateral MT–MT interactions and uses motor activity to straighten the angle between the MTs, resulting in a linear bundle. This mechanism is a variation of the classic inward force production model, wherein minus end motors cross-link antiparallel MTs and slide them together toward the spindle midzone. Accordingly, the observation of elongated prophase/prometaphase spindles in *atk5-1* plants implicates ATK5 in

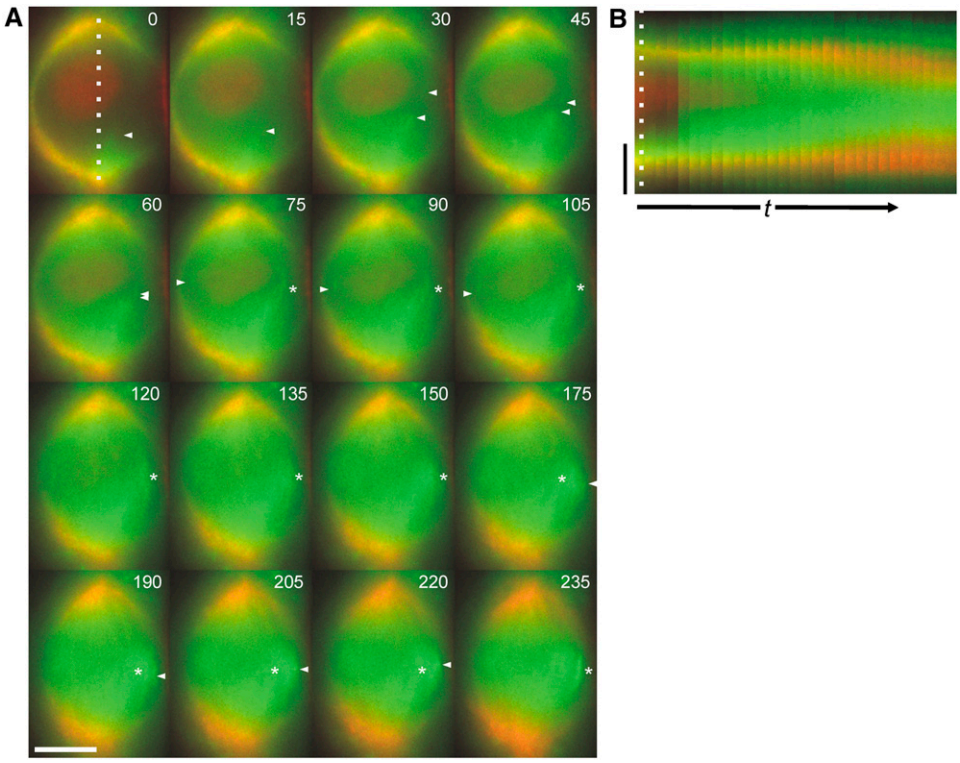

Figure 6. Localization of YFP:ATK5 (Green) and MBD:Ds Red (Red) during the Prophase-to-Prometaphase Transition in a Tobacco BY-2 Cell.

(A) Images taken from a time-lapse series (see Supplemental Movie 4 online) with 15-s intervals between frames. YFP:ATK5 moves from the poles inward (arrowheads) and becomes enriched at regions of overlap between antiparallel interpolar MT bundles (asterisks).
(B) Kymograph of the entire sequence taken along the dotted line in **(A)**.
The time scale (*t*) in **(B)** is 345 s. Bars = 10 μm.

generating inward forces, the existence of which were previously theoretical in plants. Furthermore, the less cohesive character of metaphase/anaphase spindles in *atk5-1* cells is suggestive of reduced lateral interactions between individual spindle MTs, which would predictably compromise structural integrity. We also provide evidence that ATK5 contributes to pole formation directly during prometaphase and indirectly during metaphase. The direct contribution is attributable to residual ATK5 at the poles during prometaphase, where it acts to focus them. The indirect contribution is during metaphase, when ATK5 is concentrated predominantly in the midzone, where it fosters lateral interactions that are then translated to the poles as a result of MT rigidity.

Spatiotemporal Correlation of ATK5 Localization and Activity

The effects of ATK5 loss on pole formation, inward force production, and lateral compaction are apparent during early prometaphase, when *atk5-1* spindles are elongated (as a result of reduced inward forces), bent (as a result of the lack of lateral compaction), and have splayed poles (as a result of reduced pole-focusing forces). At this stage in wild-type spindles, ATK5 is concentrated on overlapping midzone MTs, where it generates inward forces to pull the two half-spindles together and straightens misaligned MTs. At the same time, additional ATK5 also remains in the polar regions, where it focuses minus ends into poles.

It is noteworthy that the normal migration of ATK5 from poles to the midzone in *Arabidopsis* spindles during prometaphase corresponds to the broadening of the spindle into its characteristic barrel shape by metaphase, suggesting that ATK5 is a key pole determinant during prometaphase and that its progressive redistribution to the midzone leads to broad spindle poles by metaphase. Support for the idea that sequestration of kinesin-14 in the midzone results in broad poles comes from the finding that the redistribution of ATK1 (83% amino acid similarity to ATK5) antibodies from the midzone to the poles during metaphase results in highly fusiform spindles in cells lysed in the presence of ATP (Liu et al., 1996).

Although ATK5 localizes to MTs before NEB, *atk5-1* spindles do not appear deficient in pole focusing at this stage. One possible interpretation is that the inward force production function of ATK5 dominates during prophase (as suggested by the premature spindle elongation in *atk5-1* cells), whereas other factors take on the role of pole organization at this stage. Similarly, any contributions of ATK5 to pole focusing during prophase may be masked by redundant pole factors that are inactivated after NEB, thereby leaving ATK5 as the predominant pole determinant during prometaphase. The actomyosin system has been implicated

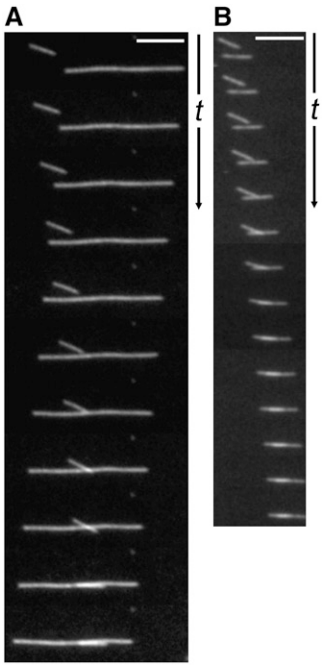

Figure 7. MTs Interact and Coalign in Vitro in the Presence of GST:ATK5 and ATP.

(A) Interaction between antiparallel MTs.
(B) Interaction between parallel MTs.
The time interval between frames is 5 s. Bars = 5 μm.

in pole organization during prophase in plant cells; specifically, disruption with cytochalasin D results in disorganized prophase spindle poles, whereas normal metaphase spindles are still able to form (Mineyuki and Palevitz, 1990; Mineyuki et al., 1991). Furthermore, the PPB also plays a role in prophase spindle pole organization, because any experimental disruption of it correlates with pole abnormalities (Mineyuki et al., 1991; Panteris et al., 1995; Nogami et al., 1996; Granger and Cyr, 2001; Camilleri et al., 2002; Chan et al., 2005; Yoneda et al., 2005). In support of this possible functional redundancy between the PPB and kinesin-14 motors, the effects of ATK1 deletion are more severe in meiotic spindles, which lack PPBs, than in mitotic spindles (Chen et al., 2002; Marcus et al., 2003). Similarly, in animal cells, the effects of kinesin-14 perturbation are often more severe in cells lacking centrosomes (which, like PPBs, spatially organize spindle MTs), such as meiotic spindles from oocytes of several species (Matthies et al., 1996; Walczak et al., 1997).

The observation that *atk5-1* prophase/prometaphase spindles begin elongation prematurely and elongate to a greater extent than do wild-type spindles is consistent with the hypothesis that ATK5 generates inward forces to counter the outward forces exerted by other kinesins, thereby acting as a brake to prevent premature spindle elongation. This finding suggests that kinesin-derived forces are present and required for normal prophase spindle formation in plants, and moreover, that a balance of inward and outward forces is required to maintain constant prophase spindle length, whereas the initiation of spindle elongation results from an imbalance favoring outward forces. Similarly, loss or depletion of the other kinesin-14 family members NCD and HSET also results in early release from stable states in animal spindles (Sharp et al., 2000; Gordon et al., 2001; Brust-Mascher and Scholey, 2002). Alternatively, another possible source of the prolonged prophase/prometaphase stage may be a deficiency in MT sorting resulting from a loss of kinesin-14–based MT–MT sliding. Indeed, numerous studies have also demonstrated slowed or less efficient spindle assembly upon the loss or depletion of kinesin-14 family members (Matthies et al., 1996; Gordon et al., 2001; Prigozhina et al., 2001; Marcus et al., 2003).

The bent prophase/prometaphase spindles seen in *atk5-1* cells are derived from cells with an initially misplaced prophase nucleus, which normally occurs in ~25% of the cells in the wild type and *atk5-1* (J.C. Ambrose and R. Cyr, unpublished observation). In several studies, bent spindles were reported when kinesin-14 proteins were disrupted (Endow and Komma, 1996; Walczak et al., 1997; Sharp et al., 2000; Prigozhina et al., 2001). To account for this effect, we propose the following model for kinesin-14 function: as MTs ingress from the poles at NEB, they encounter MTs from the opposite pole and interact to form interpolar MT bundles. However, because these MTs radiate out from discrete poles, they often encounter opposing MTs at an angle (especially in spindles with a bent axis). The presence of kinesin-14 allows opposing MTs encountering one another at angles to interact and coalign, thereby straightening the spindle axis as well as contributing to longitudinal and lateral compaction. We propose that ATK5 and perhaps other kinesin-14 family members establish lateral MT connections via a search-and-capture mechanism, similar to that seen with kinetochore–MT interactions.

The in vitro bundle formation documented here is consistent with this model, although in contrast to a mitotic spindle, MTs are not dynamic in this biochemical assay, other MT-associated proteins and regulatory proteins are absent, and stabilized MTs are gliding in a two-dimensional plane. Nevertheless, such in vitro bundle formation, in the presence of ATP, is not a prominent activity of kinesin-I proteins (J.C. Ambrose and R. Cyr, unpublished observations using *Drosophila* Dm HCK), suggesting that linear bundle formation is kinesin-14–dependent and not an artifact of the MT gliding assay per se. In addition to bent spindles, further in vivo evidence for the model is observed in the form of MT spurs extending out from the spindle upon the disruption of other kinesin-14 family members (Endow et al., 1994; Endow and Komma, 1996; Sharp et al., 1999, 2000; Gordon et al., 2001), which may result from failed capture and coalignment of MTs into interpolar bundles. Additional support for this notion is observed in *Drosophila* cells, which contain only a single kinesin-14 motor (i.e., NCD), compared with 21 predicted kinesin-14 motors in *Arabidopsis*. Although not discussed, Supplemental Movie 7 online shows Ncd RNA interference cells at prometaphase, in which the ingressing interpolar MTs appear not to interact with those growing in from the opposite pole as they reach the midzone, whereas in control cells they interact and coalign (Goshima and Vale, 2003).

By metaphase and anaphase, ATK5 exhibits strong enrichment in the spindle midzone (Ambrose et al., 2005), where it presumably generates inward forces to draw the two half-spindles together. However, metaphase and anaphase spindles

exhibited no increase in length in mutant spindles, as would be predicted from this simple model. Instead, an increase in spindle width and a loss of integrity of *atk5-1* spindles at these stages were more apparent. In agreement with our in vitro data showing ATK5-dependent MT coalignment, these phenotypes support the hypothesis that ATK5 mediates lateral interactions between MTs and uses motility to straighten discordant MTs and coalign them into a linear bundle parallel to the spindle axis. The hypothesis that ATK5 mediates lateral connections in the spindle predominantly via interpolar MTs is supported by the observation of laterally broadened, *atk5-1*–like metaphase and anaphase spindles upon treatment of dividing root cells with low levels of colchicine sufficient to remove interpolar MTs without significantly decreasing kinetochore MTs (Galatis and Apostolakos, 1991).

Only in the case of the fission yeast Klp2p has the loss of a kinesin-14 resulted in a significant increase in metaphase spindle length (Troxell et al., 2001). Metaphase spindle length in *Drosophila* cells is minimally affected in response to perturbations of force-generating motors; instead, MT dynamics play the dominant role in governing metaphase spindle length (Goshima et al., 2005). Indeed, MT dynamics have been implicated in governing metaphase spindle length in plant cells as well (Kawamura et al., 2006). One explanation for why *atk5-1* exhibits spindle length increases in prophase/prometaphase, but not during metaphase and anaphase, is that prophase/prometaphase spindles lack the well-defined kinetochore fibers that are present later on in metaphase and anaphase. Anchoring of kinetochore fibers to chromosomes at the metaphase plate may supersede the interpolar MTs in maintaining spindle length via dynamic modulations of poleward flux rates. Furthermore, the establishment of kinetochore fibers during metaphase may also contribute to the straightening of the bent prometaphase spindles seen in *atk5-1* cells.

Mode of Midzone Accumulation

We previously hypothesized that the plus end tracking of ATK5 might be responsible for its accumulation at the spindle midzone, but we have been unable to observe any plus end tracking of ATK5 during mitosis. We report here that during MT ingression at NEB/prometaphase, YFP:ATK5 signal moves from the poles inward on MTs and becomes enriched at regions of overlap between opposing interpolar MTs as antiparallel connections are established. Hence, the midzone enrichment may not be a result of plus end tracking per se but rather a manifestation of an increased affinity for neighboring plus ends in an antiparallel orientation; this plus end affinity is also evident during interphase in the form of plus end tracking. Interestingly, the lateral interactions observed in our in vitro assays were both parallel and antiparallel, suggesting that the in vivo preference of antiparallel ATK5 association is the result of fine-tuning via additional plus end components.

Evidence that ATK5 preferentially localizes to overlapping regions of interpolar MT bundles is threefold: (1) midzone enrichment is strongest when MTs congressing from the poles have reached and crossed the midzone; (2) interpolar MT bundles typically extend from the pole regions to the midzone, where they overlap with interpolar bundles from the opposite pole to form continuous bundles (Jensen and Bajer, 1973; Euteneuer and McIntosh, 1980; Euteneuer et al., 1982); by contrast, ATK5 localizes only to short (2 to 3 μm) segments spanning the midzone within these long interpolar MT bundles extending toward the poles (Figures 4 to 7); and (3) the midzone fluorescence of YFP:ATK5 persists throughout anaphase, becoming constricted laterally and shortening as the region of overlap between MT decreases as a result of MT sliding (Euteneuer et al., 1982; Baskin and Cande, 1990). Whether ATK5 itself specifically cross-links antiparallel MTs or it recognizes a protein or complex in these regions warrants further investigation. We currently favor the latter scenario, because removal of the ATK5 motor domain does not interfere with its midzone accumulation (Ambrose et al., 2005).

METHODS

Plant Material and Growth Conditions

Arabidopsis thaliana plant growth, cell culture maintenance, and *Agrobacterium tumefaciens*–mediated stable transformations were performed as described previously (Ambrose et al., 2005). Plasmid containing GFP:TUB6 was a gift from T. Hashimoto (Nara Institute of Science and Technology) and was stably transformed into wild-type and *atk5-1* plants. For live observation of plants expressing GFP:TUB6, single-well chamber slides (Sigma-Aldrich) supplemented with a 3-mm layer of growth medium were used. Seeds were pushed through the medium with a sterile toothpick until they reached the cover slip at the bottom of the chamber. Chambers were then placed at an angle, allowing for the observation of roots as they grew along the agar–cover slip interface. Seedlings were observed for 3 to 7 d after germination.

Fluorescence Microscopy and Image Analysis

Images were collected using a Plan-Neofluar 40× (numerical aperture 1.3) oil-immersion objective (Zeiss). Wide-field microscopy was conducted using a shutter-equipped Zeiss Axiovert microscope, and images were captured with a Coolsnap HQ CCD camera (Roper Industries) controlled by ESEE software (Inovision). To distinguish between fluorophores, the following filter sets were used: GFP (460- to 500-nm excitation, 510- to 560-nm emission), YFP (490- to 510-nm excitation, 520- to 550-nm emission), and Ds Red (530- to 560-nm excitation, 575- to 645-nm emission). Intervals used during time-lapse imaging ranged from 15 s to 1 min and are indicated in the figures. Typical exposure times were 1 to 2 s. Image analyses were performed using ImageJ software (http://rsb.info.nih.gov/ij/).

Confocal Microscopy

Confocal imaging was performed with a 40× Plan-Apochromatic water-immersion objective mounted on a Zeiss LSM 510 microscope, using a 488-nm argon laser. GFP fluorescence was observed using a 488-nm dichroic filter and a 505- to 545-nm emission filter. Typical scan times were 4 s, using a line averaging of two. Scan intervals were variable and are indicated in the figure legends.

In Vitro Motility Assays

Cleared bacterial lysates from BL21 (DE3) cells (Novagen) expressing GST:ATK5 were used. MT gliding assays were done as described previously (Marcus et al., 2002), with the modification that the MT solution was mixed 1:10 with GST:ATK5 lysates immediately before viewing.

Accession Number

The Arabidopsis Genome Initiative locus identifier for *ATK5* is At4g05190.

Supplemental Data

The following materials are available in the online version of this article.

Supplemental Table 1. Behavior and Morphology of Mitotic Spindles Are Unaffected in Plants Expressing YFP:ATK5.

Supplemental Figure 1. Bundle Formation by GST:ATK5.

Supplemental Movie 1. Mitosis in the Root Tip of a Wild-Type Plant Expressing GFP:TUB6.

Supplemental Movie 2. Mitosis in the Root Tip of an *atk5-1* Plant Expressing GFP:TUB6.

Supplemental Movie 3. YFP:ATK5 Is Enriched on Interpolar MTs in Early Prometaphase in Tobacco BY-2 Cells.

Supplemental Movie 4. YFP:ATK5 Moves from the Pole to the Midzone during Prometaphase and Becomes Enriched in Regions of Overlap between Antiparallel Interpolar MT Bundles.

ACKNOWLEDGMENTS

We thank D. Fisher for critical reading of the manuscript, T. Hashimoto for the generous gift of GFP:TUB6, and the Salk Institute Genomic Analysis Laboratory for providing the sequence-indexed *Arabidopsis* T-DNA insertion mutants. This work was funded by grants from the USDA, the Department of Energy, and the National Science Foundation.

Received September 22, 2006; revised October 28, 2006; accepted November 13, 2006; published January 12, 2007.

REFERENCES

Ambrose, J.C., Li, W., Marcus, A., Ma, H., and Cyr, R. (2005). A minus-end-directed kinesin with plus-end tracking protein activity is involved in spindle morphogenesis. Mol. Biol. Cell **16:** 1584–1592.

Arabidopsis Genome Initiative (2000). Analysis of the genome sequence of the flowering plant *Arabidopsis thaliana*. Nature **408:** 796–815.

Bajer, A.S., and Molè-Bajer, J. (1986). Reorganization of microtubules in endosperm cells and cell fragments of the higher-plant *Haemanthus* in vivo. J. Cell Biol. **102:** 263–281.

Baskin, T.I., and Cande, W.Z. (1990). The structure and function of the mitotic spindle in flowering plants. Annu. Rev. Plant Physiol. Plant Mol. Biol. **41:** 277–315.

Brust-Mascher, I., and Scholey, J.M. (2002). Microtubule flux and sliding in mitotic spindles of Drosophila embryos. Mol. Biol. Cell **13:** 3967–3975.

Camilleri, C., Azimzadeh, J., Pastuglia, M., Bellini, C., Grandjean, O., and Bouchez, D. (2002). The Arabidopsis TONNEAU2 gene encodes a putative novel protein phosphatase 2A regulatory subunit essential for the control of the cortical cytoskeleton. Plant Cell **14:** 833–845.

Chan, J., Calder, G., Fox, S., and Lloyd, C. (2005). Localization of the microtubule end binding protein EB1 reveals alternative pathways of spindle development in Arabidopsis suspension cells. Plant Cell **17:** 1737–1748.

Chen, C., Marcus, A., Li, W., Hu, Y., Calzada, J.P., Grossniklaus, U., Cyr, R.J., and Ma, H. (2002). The Arabidopsis ATK1 gene is required for spindle morphogenesis in male meiosis. Development **129:** 2401–2409.

Dagenbach, E.M., and Endow, S.A. (2004). A new kinesin tree. J. Cell Sci. **117:** 3–7.

Dixit, R., and Cyr, R. (2004). Encounters between dynamic cortical microtubules promote ordering of the cortical array through angle-dependent modifications of microtubule behavior. Plant Cell **16:** 3274–3284.

Endow, S.A., Chandra, R., Komma, D.J., Yamamoto, A.H., and Salmon, E.D. (1994). Mutants of the Drosophila ncd microtubule motor protein cause centrosomal and spindle pole defects in mitosis. J. Cell Sci. **107:** 859–867.

Endow, S.A., and Komma, D.J. (1996). Centrosome and spindle function of the Drosophila Ncd microtubule motor visualized in live embryos using Ncd-GFP fusion proteins. J. Cell Sci. **109:** 2429–2442.

Euteneuer, U., Jackson, W.T., and McIntosh, J.R. (1982). Polarity of spindle microtubules in Haemanthus endosperm. J. Cell Biol. **94:** 644–653.

Euteneuer, U., and McIntosh, J.R. (1980). Polarity of midbody and phragmoplast microtubules. J. Cell Biol. **87:** 509–515.

Galatis, B., and Apostolakos, P. (1991). Patterns of microtubule reappearance in root cells of *Vigna sinensis* recovering from a colchicine treatment. Protoplasma **160:** 131–143.

Gordon, M.B., Howard, L., and Compton, D.A. (2001). Chromosome movement in mitosis requires microtubule anchorage at spindle poles. J. Cell Biol. **152:** 425–434.

Goshima, G., and Vale, R.D. (2003). The roles of microtubule-based motor proteins in mitosis: Comprehensive RNAi analysis in the Drosophila S2 cell line. J. Cell Biol. **162:** 1003–1016.

Goshima, G., Wollman, R., Stuurman, N., Scholey, J.M., and Vale, R.D. (2005). Length control of the metaphase spindle. Curr. Biol. **15:** 1979–1988.

Granger, C., and Cyr, R. (2001). Use of abnormal preprophase bands to decipher division plane determination. J. Cell Sci. **114:** 599–607.

Jensen, C., and Bajer, A.S. (1973). Spindle dynamics and arrangement of microtubules. Chromosoma **44:** 73–89.

Karabay, A., and Walker, R.A. (1999). Identification of microtubule binding sites in the Ncd tail domain. Biochemistry **38:** 1838–1849.

Kawamura, E., Himmelspach, R., Rashbrooke, M.C., Whittington, A.T., Gale, K.R., Collings, D.A., and Wasteneys, G.O. (2006). MICROTUBULE ORGANIZATION 1 regulates structure and function of microtubule arrays during mitosis and cytokinesis in the Arabidopsis root. Plant Physiol. **140:** 102–114.

Liu, B., Cyr, R.J., and Palevitz, B.A. (1996). A kinesin-like protein, KatAp, in the cells of Arabidopsis and other plants. Plant Cell **8:** 119–132.

Marcus, A.I., Ambrose, J.C., Blickley, L., Hancock, W.O., and Cyr, R.J. (2002). *Arabidopsis thaliana* protein, ATK1, is a minus-end directed kinesin that exhibits non-processive movement. Cell Motil. Cytoskeleton **52:** 144–150.

Marcus, A.I., Li, W., Ma, H., and Cyr, R.J. (2003). A kinesin mutant with an atypical bipolar spindle undergoes normal mitosis. Mol. Biol. Cell **14:** 1717–1726.

Matthies, H.J., McDonald, H.B., Goldstein, L.S., and Theurkauf, W.E. (1996). Anastral meiotic spindle morphogenesis: Role of the non-claret disjunctional kinesin-like protein. J. Cell Biol. **134:** 455–464.

McDonald, H.B., Stewart, R.J., and Goldstein, L.S. (1990). The kinesin-like ncd protein of Drosophila is a minus end-directed microtubule motor. Cell **63:** 1159–1165.

Mineyuki, Y., Marc, J., and Palevitz, B.A. (1991). Relationship between the preprophase band, nucleus and spindle in dividing Allium cotyledon cells. J. Plant Physiol. **138:** 640–649.

Mineyuki, Y., and Palevitz, B.A. (1990). Relationship between preprophase band organization, F-actin and the division site in Allium—Fluorescence and morphometric studies on cytochalasin-treated cells. J. Cell Sci. **97:** 283–295.

Mountain, V., Simerly, C., Howard, L., Ando, A., Schatten, G., and Compton, D.A. (1999). The kinesin-related protein, HSET, opposes the activity of Eg5 and cross-links microtubules in the mammalian mitotic spindle. J. Cell Biol. **147:** 351–366.

Murata, T., Sonobe, S., Baskin, T.I., Hyodo, S., Hasezawa, S., Nagata, T., Horio, T., and Hasebe, M. (2005). Microtubule-dependent microtubule nucleation based on recruitment of gamma-tubulin in higher plants. Nat. Cell Biol. **10:** 961–968.

Narasimhulu, S.B., and Reddy, A.S. (1998). Characterization of microtubule binding domains in the Arabidopsis kinesin-like calmodulin binding protein. Plant Cell **10:** 957–965.

Nogami, A., Suzaki, T., Shigenaka, Y., Nagahama, Y., and Mineyuki, Y. (1996). Effects of cycloheximide on preprophase bands and prophase spindles in onion (*Allium cepa* L) root tip cells. Protoplasma **192:** 109–121.

O'Connell, M.J., Meluh, P.B., Rose, M.D., and Morris, N.R. (1993). Suppression of the bimC4 mitotic spindle defect by deletion of klpA, a gene encoding a KAR3-related kinesin-like protein in *Aspergillus nidulans*. J. Cell Biol. **120:** 153–162.

Palevitz, B.A. (1988). Microtubular fir-trees in mitotic spindles of onion roots. Protoplasma **142:** 74–78.

Panteris, E., Apostolakos, P., and Galatis, B. (1995). The effect of taxol on Triticum preprophase root-cells—Preprophase microtubule band organization seems to depend on new microtubule assembly. Protoplasma **186:** 72–78.

Prigozhina, N.L., Walker, R.A., Oakley, C.E., and Oakley, B.R. (2001). Gamma-tubulin and the C-terminal motor domain kinesin-like protein, KLPA, function in the establishment of spindle bipolarity in *Aspergillus nidulans*. Mol. Biol. Cell **12:** 3161–3174.

Richardson, D.N., Simmons, M.P., and Reddy, A.S. (2006). Comprehensive comparative analysis of kinesins in photosynthetic eukaryotes. BMC Genomics **7:** 18.

Sharp, D.J., Brown, H.M., Kwon, M., Rogers, G.C., Holland, G., and Scholey, J.M. (2000). Functional coordination of three mitotic motors in Drosophila embryos. Mol. Biol. Cell **11:** 241–253.

Sharp, D.J., Yu, K.R., Sisson, J.C., Sullivan, W., and Scholey, J.M. (1999). Antagonistic microtubule-sliding motors position mitotic centrosomes in Drosophila early embryos. Nat. Cell Biol. **1:** 51–54.

Smirnova, E.A., Reddy, A.S.N., Bowser, J., and Bajer, A.S. (1998). Minus end-directed kinesin-like motor protein, Kcbp, localizes to anaphase spindle poles in Haemanthus endosperm. Cell Motil. Cytoskeleton **41:** 271–280.

Surrey, T., Nedelec, F., Leibler, S., and Karsenti, E. (2001). Physical properties determining self-organization of motors and microtubules. Science **292:** 1167–1171.

Troxell, C.L., Sweezy, M.A., West, R.R., Reed, K.D., Carson, B.D., Pidoux, A.L., Cande, W.Z., and McIntosh, J.R. (2001). pkl1(+) and klp2(+): Two kinesins of the Kar3 subfamily in fission yeast perform different functions in both mitosis and meiosis. Mol. Biol. Cell **12:** 3476–3488.

Vos, J.W., Dogterom, M., and Emons, A.M.C. (2004). Microtubules become more dynamic but not shorter during preprophase band formation: A possible ''search-and-capture'' mechanism for microtubule translocation. Cell Motil. Cytoskeleton **57:** 246–258.

Walczak, C.E., Verma, S., and Mitchison, T.J. (1997). XCTK2: A kinesin-related protein that promotes mitotic spindle assembly in *Xenopus laevis* egg extracts. J. Cell Biol. **136:** 859–870.

Walczak, C.E., Vernos, I., Mitchison, T.J., Karsenti, E., and Heald, R. (1998). A model for the proposed roles of different microtubule-based motor proteins in establishing spindle bipolarity. Curr. Biol. **8:** 903–913.

Walker, R.A., Salmon, E.D., and Endow, S.A. (1990). The Drosophila claret segregation protein is a minus-end directed motor molecule. Nature **347:** 780–782.

Wick, S.M., and Duniec, J. (1983). Immunofluorescence microscopy of tubulin and microtubule arrays in plant cells. I. Preprophase band development and concomitant appearance of nuclear envelope-associated tubulin. J. Cell Biol. **97:** 235–243.

Yoneda, A., Akatsuka, M., Hoshino, H., Kumagai, F., and Hasezawa, S. (2005). Decision of spindle poles and division plane by double preprophase bands in a BY-2 cell line expressing GFP-tubulin. Plant Cell Physiol. **46:** 531–538.

Zhu, C., Zhao, J., Bibikova, M., Leverson, J.D., Bossy-Wetzel, E., Fan, J.B., Abraham, R.T., and Jiang, W. (2005). Functional analysis of human microtubule-based motor proteins, the kinesins and dyneins, in mitosis/cytokinesis using RNA interference. Mol. Biol. Cell **16:** 3187–3199.